International Conference on Non-conventional Materials and Technologies
NOCMAT 2022

ANALYTICAL PREDICTION OF FAILURE MECHANISM AND FAILURE MOMENT IN FULL-CULM BAMBOO BENDING TESTS

Theodora Mouka, The Hong Kong University of Science and Technology, Hong Kong, tmouka@connect.ust.hk
Elias G. Dimitrakopoulos, The Hong Kong University of Science and Technology, Hong Kong, ilias@ust.hk
Rodolfo Lorenzo, University College London, UK, r.lorenzo@ucl.ac.uk

ABSTRACT
This study determines analytically the critical failure mechanisms that lead to bamboo culm bending failure, and predicts the failure moment. Specifically, the study examines four distinct failure mechanisms: Brazier instability, longitudinal tension/compression, tension perpendicular to the fibers, and shear parallel to the fibers. After identifying the critical failure mechanisms, the study utilizes the derived analytical expressions to predict the failure moment for three bamboo species; i.e., Moso, Guadua and Kao Jue. It compares the analytical predictions to experimental results, concluding that the proposed equations are sufficiently accurate in their prediction of failure moment, although they tend to slightly underestimate it.

KEYWORDS
Full-culm bamboo; bending test; failure map; failure mechanisms.

INTRODUCTION
Bamboo has been increasingly popular as a structural material in recent decades, because of its cost-efficiency, high strength-to-weight ratio (Janssen, 1981), and sustainability (Wu et al., 2015). However, currently there is incomplete understanding on bamboo structural member behavior, and especially on full-culm bamboo flexural members.

Full-culm bamboo flexural members exhibit intricate behavior, because of the tubular culm shape and bamboo morphology (Wang et al., 2012, Dixon & Gibson, 2014, Mannan et al., 2017, Akinbade et al., 2019), which resembles a uni-directional fiber-reinforced composite (Amada et al., 1997). Hence, bamboo culms subjected to bending can fail in various ways, such as longitudinal splitting, culm wall buckling, or culm collapse (Trujillo et al., 2017). These are all common failure modes observed experimentally, yet bamboo testing standards (e.g., ISO 22157:2019) dictate that they should be avoided, while bamboo design standards (e.g., ISO 22156:2021) specify bamboo culm geometric characteristics to prevent them.

The underlying mechanisms behind these failure modes are unclear. For example, some studies attribute longitudinal splitting to circumferential tension (Lorenzo et al., 2021, Wegst & Ashby, 2007, Mitch et al., 2010, Sharma et al. 2013), while others to shear, or shear-circumferential tension interaction (Trujillo et al., 2017, Richard et al., 2017). The uncertainty on failure mode underlying mechanisms, combined with the fact that bamboo culm modulus of rupture (MOR) is case-specific (as it depends on culm geometry and density, e.g., Gnanaharan et al., 1995), complicate the development of a universal approach to determine the failure load of full-culm bamboo flexural members.

This study aims to identify the critical failure modes and provide analytical tools for the prediction of the failure load of bamboo culms subjected to bending. Thus, the study aims to facilitate the rational engineering design of bamboo structures.

FAILURE MECHANISMS AND CRITICAL BENDING MOMENT

This section examines four potential failure mechanisms of bamboo culms subjected to bending, namely; Brazier instability, longitudinal tension/compression, longitudinal splitting induced by circumferential tension, and shear-induced longitudinal splitting. The section calculates the critical bending moment at which each of the failure modes occurs (fig. 1a), as a function of culm geometry and material properties. Culm geometry is taken into account via the culm shape factor ϕ (Wegst & Ashby, 2007), equal to the ratio of culm midline radius to thickness:

$$\phi = \frac{R}{t} \qquad \text{Eq. 1}$$

Shape factor ϕ associates with the ratio of culm external diameter D_o to thickness t as:

$$\frac{D_o}{t} = 2\phi + 1 \qquad \text{Eq. 2}$$

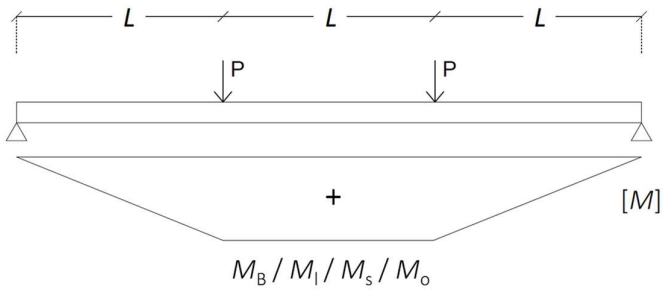

a) Bending moments for each of the failure mechanisms (typical four-point bending test)

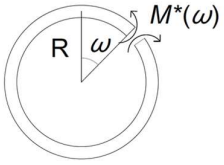

b) Bending moment that causes bending in the cross-section plane

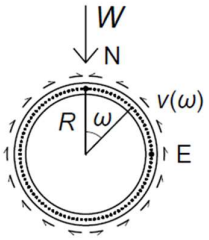

c) Assumed cross-section loading

Figure 1: Notation of bending moments and cross-section loading.

The first failure mechanism under consideration is Brazier instability (Brazier & Southwell, 1927). Specifically, when a circular tube is subjected to bending, its cross-section tends to ovalize, ultimately causing local kinking of the tube. This happens at a critical value of the bending moment (Brazier moment, M_B). That critical value for an orthotropic tube is (Wegst & Ashby, 2007):

$$\frac{M_B}{A^{1.5}} = \frac{1}{9\sqrt{\pi}}\sqrt{\frac{E_{\parallel}E_{\perp}}{\phi}} \qquad \text{Eq. 3}$$

where ϕ is the culm shape factor (eq. 1), $A = 2\pi Rt$ is the tube cross-section area, $E_{\parallel}$ the longitudinal Young's modulus and $E_{\perp}$ the transverse Young's modulus.

Further, the critical bending moment for failure in the longitudinal direction (M_l) —in tension or compression— is (Wegst & Ashby, 2007):

$$\frac{M_l}{A^{1.5}} = \frac{1}{\sqrt{8\pi}} \sigma_{u\|} \sqrt{\phi} \qquad \text{Eq. 4}$$

where $\sigma_{u\|}$ is the tensile or compressive strength (whichever is lower) in the longitudinal direction.

For longitudinal splitting because of shear, consider a three-point or a four-point bending test (e.g., fig. 1a), which are the most common bending test configurations for bamboo. The critical bending moment for shear-induced splitting (M_s) at a load application point is (Mouka et al, 2022):

$$\frac{M_s}{A^{1.5}} = \frac{n\tau_{u\|}\sqrt{2}}{\left(2+\frac{1}{\phi}\right)\sqrt{\pi}} \sqrt{\phi} \qquad \text{Eq. 5}$$

where $\tau_{u\|}$ is the shear strength parallel to the fibers and $n = L/(2R)$ a parameter introduced by Mouka et al, 2022, that denotes the normalized with culm midline diameter shear span length (L denotes the shear span length, fig. 1a).

Finally, for splitting induced by circumferential tension, we associate the bending moment in the plane of the cross-section (i.e., the moment that causes the circumferential tension, M^*, fig. 1b) with culm ovalization, and subsequently associate ovalization with the bending moment M_o that is its origin (bending moment M_o causes bending in the longitudinal direction, fig. 1a). Bending moment M^* depends on the assumed loading in the plane of the cross-section. Consider the loading of fig. 1c, which involves a point load W resisted by a shear flow $v(\omega)$ along the culm circumference (where ω is the angular coordinate along the circumference, fig. 1c). The assumed shear flow distribution is as follows:

$$v(\omega) = \frac{W \sin\omega}{\pi R} \qquad \text{Eq. 6}$$

The resulting bending moment M^* (fig. 1b) that causes bending in the cross-section plane is (Young & Budynas, 2002):

$$M^*(\omega) = \frac{WR}{2\pi}\left[1+\frac{1}{2}\cos\omega-(\pi-\omega)\sin\omega\right] \qquad \text{Eq. 7}$$

Subsequently, following the procedure described in Wegst & Ashby, 2007, and taking into account eq. 7, the critical bending moment at which circumferential-tension-induced splitting occurs (M_o, fig. 1a) is (Mouka et al. 2022):

$$M_o = 0.1114\sqrt{E_{\|}\sigma_{\perp u}}\left(1-0.4680\frac{\sigma_{\perp u}}{E_{\perp}}\phi\right) \qquad \text{Eq. 8}$$

where $\sigma_{\perp u}$ is the tensile strength in the circumferential direction (perpendicular to the fibers).

Failure map

After deriving analytical expressions for the failure moment of each failure mechanism, this study constructs "failure maps" for three bamboo species —i.e., Moso (*Phyllostachys pubescens*), Guadua

(*Guadua angustifolia* Kunth) and Kao Jue (*Bambusa pervariabilis*)— to determine the critical failure mechanism of each species (fig. 2). The failure maps illustrate the critical bending moment as a function of shape factor ϕ (eq. 1) or, alternatively, the ratio of external diameter to thickness (eq. 2). Table 1 lists the material properties adopted in the failure maps. Figure 2 shows that Brazier instability and shear-induced longitudinal splitting are not critical failure modes for typical material property values of the bamboo species under consideration. Regarding the remaining failure modes, Moso is more likely to fail in circumferential tension, while Kao Jue in longitudinal compression. Guadua can fail in either of the two mechanisms, depending on the culm shape factor. The critical shape factor that marks the change of failure mode from longitudinal compression to circumferential tension occurs from eqs. 4 and 8:

$$\phi_{cr} = \left[1.068 \frac{E_{\perp}}{\sigma_{\perp u}} \left(\sqrt{10.073 \frac{\sigma_{u\parallel}^{\,2}}{\pi E_{\parallel} \sigma_{\perp u}} + 1.872 \frac{\sigma_{\perp u}}{E_{\perp}}} - 3.174 \frac{\sigma_{u\parallel}}{\sqrt{\pi E_{\parallel} \sigma_{\perp u}}} \right) \right]^2 \quad \text{Eq. 9}$$

When $\phi < \phi_{cr}$, failure occurs by longitudinal compression, and, when $\phi > \phi_{cr}$, failure occurs by tension perpendicular to the fibers.

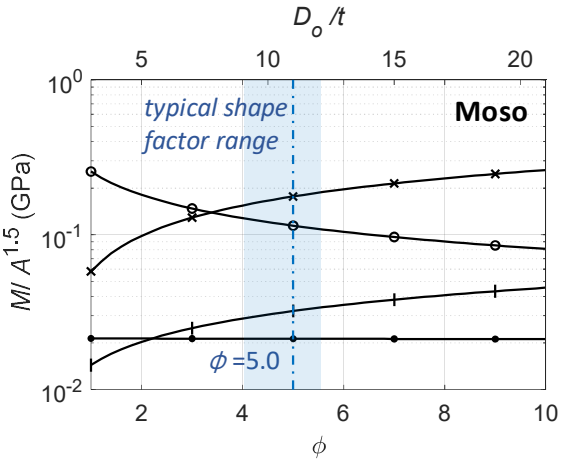

a) Failure map for Moso

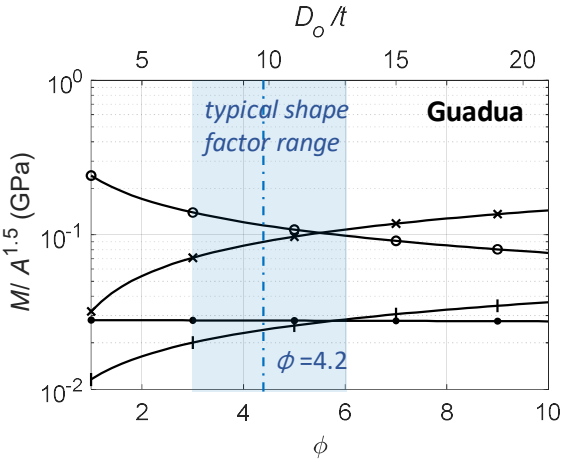

b) Failure map for Guadua

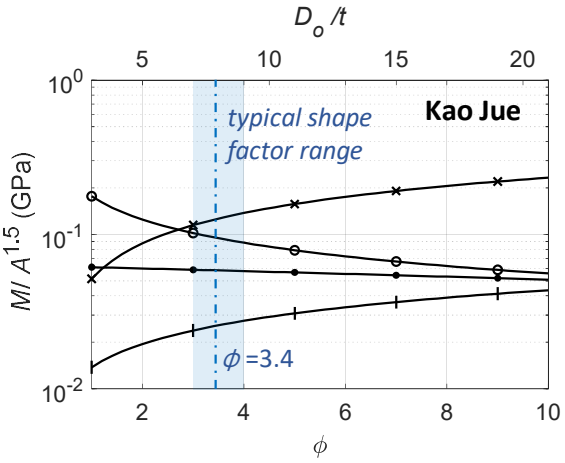

c) Failure map for Kao Jue

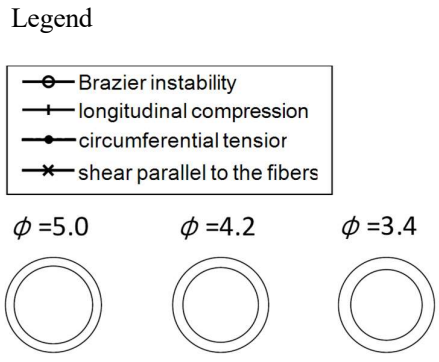

Figure 2: Failure maps (normalized critical moment versus shape factor ϕ or external radius to thickness ratio D_o/t) for Moso, Guadua, and Kao Jue. The depicted curve for shear parallel to the fibers assumes normalized shear span length n=10.

Table 1: Bamboo material properties adopted in the failure maps (property values in MPa)

	Moso		Guadua		Kao Jue	
	value	study	value	study	value	study
$E_{\parallel}$	12320	Lorenzo et al., 2021	17204	Trujillo et al., 2017	18500	Chung & Yu, 2002
$E_{\perp}$	1355	Moran et al., 2017	864	Moran et al., 2017	429	Mouka & Dimitrakopoulos, 2021
$\sigma_{u\parallel}$	72.2	Lorenzo et al., 2021	58.0	Lorenzo et al., 2020	69.0	Chung & Yu, 2002
$\sigma_{\perp u}$	3.0	Lorenzo et al., 2021	3.7	Moran et al., 2017	17.0	Mouka & Dimitrakopoulos, 2021
$\tau_{u\parallel}$	21.8	Lorenzo et al., 2021	12.0	Lorenzo et al., 2020	19.4	Paraskeva et al., 2017

Figure 3 plots ϕ_{cr} as a function of the dimensionless parameters $E_{\perp}/\sigma_{\perp u}$ and $\sigma_{u\parallel}/\left(E_{\parallel}\sigma_{\perp u}\right)$ (eq. 9) for typical bamboo material properties. It shows that ϕ_{cr} is practically independent of ratio $E_{\perp}/\sigma_{\perp u}$, except for low values of $E_{\perp}/\sigma_{\perp u}$ (approximately lower than 80). Low value of $E_{\perp}/\sigma_{\perp u}$ in practice means high circumferential tensile strength compared to the circumferential Young's modulus, as for example is the case for Kao Jue (Table 1).

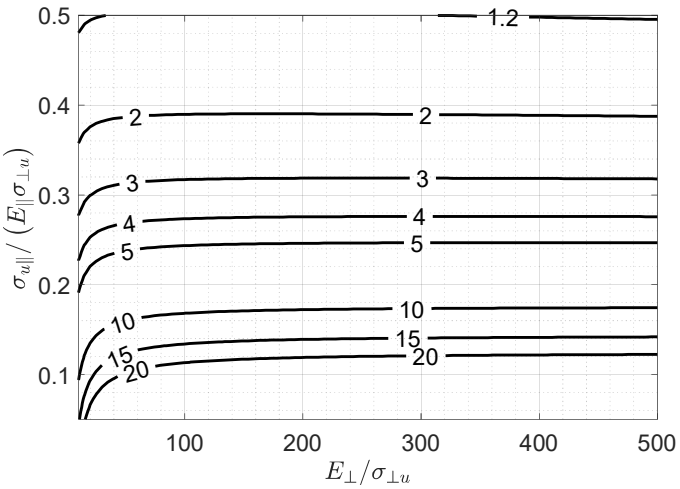

Figure 3: Critical shape factor ϕ_{cr} as a function of dimensionless parameters $E_{\perp}/\sigma_{\perp u}$ and $\sigma_{u\parallel}/\left(E_{\parallel}\sigma_{\perp u}\right)$ (eq. 9).

COMPARISON WITH EXPERIMENTAL RESULTS

This section verifies the predictions of the herein derived equations with pertinent experimental results for the three bamboo species under consideration. For Moso, we consider the four-point bending experimental results of Lorenzo et al., 2021. Figure 4b compares the prediction of eq. 8 with the maximum experimental load F_{max} and a nominal experimental failure load F_u. F_u occurs from the experimental force-displacement curves, as the force at the intersection of two lines: the first line is defined by the experimental datapoints at 20% and 60% of the maximum load F_{max} (presumed elastic region, ISO22157:2019), and the second line by the datapoints at 90% and 100% of the maximum load F_{max} (fig. 4a). The results of fig. 4b adopt actual values of $E_{\parallel}$ and ϕ for each specimen (according to

the pertinent study), and show that eq. 8 predicts F_u with sufficient accuracy (average absolute error 8%), but it underestimates F_{max}.

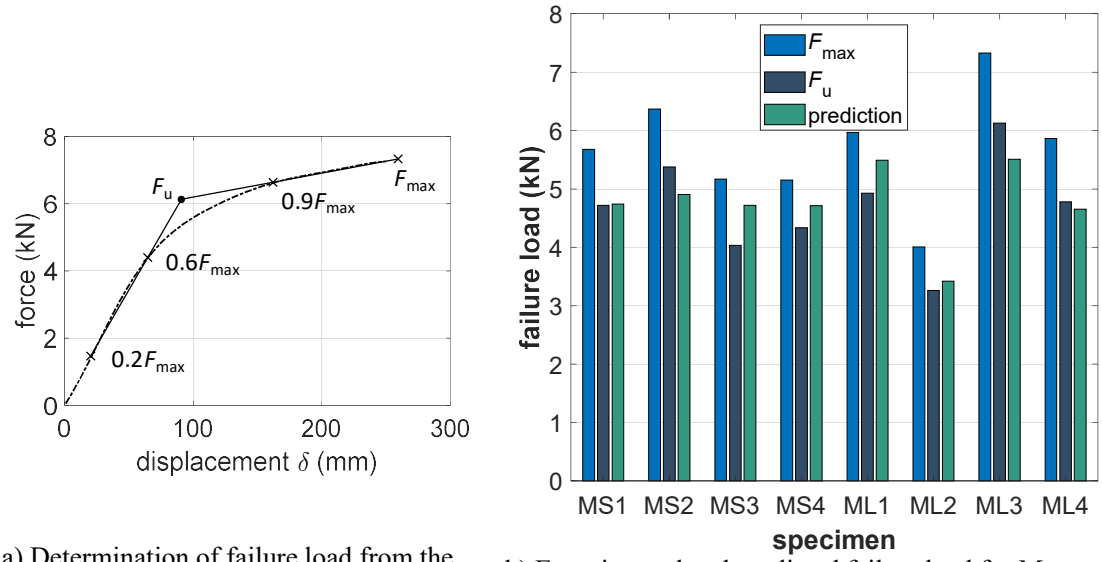

a) Determination of failure load from the experimental force-displacement curve

b) Experimental and predicted failure load for Moso

Figure 4: Comparison between experimental and predicted failure load for Moso (experimental data: Lorenzo et al 2021).

For Guadua, fig. 5 compares the predictions of the herein derived equations with the four-point bending experimental results of Trujillo et al., 2017. The predicted values occur utilizing actual specimen geometrical data and average material properties (Table 1). The predicted failure moment occurs as the minimum of eqs. 4 and 8. Predicted and experimental results exhibit similar correlations between failure moment and external diameter (fig. 5). However, the analytical prediction tends to underestimate the experimental values (by 18% on average). A reason for this is that the predicted failure moment refers to the bending moment of failure initiation and not to the maximum bending moment (M_{max}), which occurs after failure initiation.

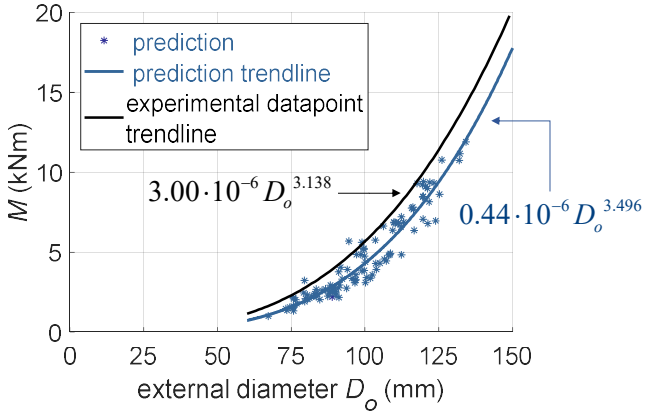

Figure 5: Comparison between experimental and predicted failure load for Guadua (experimental trendline: Trujillo et al 2017).

Regarding Kao Jue, experimental data of bending tests are scarce. Table 2 compares the failure moment predicted by this study (eq. 4) with average experimental values of Chung & Yu, 2002 and Paraskeva

et al, 2017. The results indicate that, adopting average material and geometrical properties, the herein developed equations accurately predict the average experimental values, underestimating them only slightly (by 2.5% to 3.5%).

Table 2: Evaluation of failure moment prediction for Kao Jue

study	$E_{\parallel}$ (MPa)	experimental failure moment M_u (kNm)	predicted failure moment M_f (kNm)	error $\frac{M_f - M_u}{M_u}$
Chung & Yu, 2002	18500	0.368	0.355	-3.5%
Paraskeva et al., 2017	12104	0.371	0.361	-2.6%

CONCLUSIONS

Full-culm bamboo flexural behavior is complex, as it depends on numerous factors (e.g., culm geometry, material properties, various failure modes). The present study identifies the critical failure mechanisms of bamboo culms subjected to bending, and develops analytical expressions for the prediction of the failure load. Considering typical material and geometrical properties for three bamboo species (Moso, Guadua, and Kao Jue), the study concludes that critical failure mode for Moso is splitting induced by circumferential tension, while Kao Jue is most likely to fail in longitudinal compression. Guadua can fail in either of the two, depending on culm shape factor (ratio of midline radius to thickness). An evaluation of the proposed analytical expressions with pertinent experimental results indicates that the analytical expressions are sufficiently accurate in their predictions, although they tend to underestimate the failure load. Overall, the present study provides analytical tools for the rational engineering design of full-culm bamboo flexural members, which is an important step towards a wider adoption of bamboo in construction.

ACKNOWLEDGEMENTS

The work presented in this paper was supported by the Research Grant Council of Hong Kong, under Grant Reference Number GRF 16213321

CONFLICT OF INTEREST

The authors declare that they have no conflicts of interest associated with the work presented in this paper.

DATA AVAILABILITY

No data was assembled for the production of this paper.

REFERENCES

[1]. Akinbade, Y. , Harries, K. A., Flower, C. V., Nettleship, I., Papadopoulos, C., Platt, S. (2019). Through-culm wall mechanical behaviour of bamboo. *Construction and Building Materials*, 216, 485–495. https://doi.org/10.1016/j.conbuildmat.2019.04.214

[2]. Amada, S., Ichikawa, Y., Munekata, T., Nagase, Y., Shimizu, H. (1997). Fiber texture and mechanical graded structure of bamboo. *Composites Part B: Engineering*, *28*(1) 13–20, https://doi.org/10.1016/S1359-8368(96)00020-0

[3]. Brazier, L. G., Southwell, R. V. (1927). On the flexure of thin cylindrical shells and other "thin" sections. *Proceedings of the Royal Society of London. Series A, Containing Papers of a Mathematical and Physical Character*, *116*(773) 104–114. https://doi.org/10.1098/rspa.1927.0125

[4]. Chung, K., Yu, W. (2002). Mechanical properties of structural bamboo for bamboo scaffoldings. *Engineering Structures*, *24*(4), 429 – 442. https://doi.org/10.1016/S0141-0296(01)00110-9

[5]. Dixon, P. G., Gibson, L. J. (2014). The structure and mechanics of Moso bamboo material. *Journal of The Royal Society Interface*, *11*(99), 20140321. https://doi.org/10.1098/rsif.2014.0321

[6]. Gnanaharan, R., Janssen, J. J., Arce, O. A. (1995). *Bending strength of Guadua bamboo: comparison of different testing procedures*. New Delhi: International Network of Bamboo and Rattan.
[7]. ISO 22156:2021(E). *Bamboo structures - Bamboo culms -Structural design.* International Organization for Standardization.
[8]. ISO 22157:2019(E). *Bamboo Structures - Determination of physical and mechanical properties of bamboo culms- Test methods*. International Organization for Standardization.
[9]. Janssen, J. A. A. (1981). *Bamboo in building structures*, Ph.D. thesis, University of Eindhoven.
[10].Lorenzo, R., Godina, M., Mimendi, L., Li, H. (2020). Determination of the physical and mechanical properties of Moso, Guadua and Oldhamii bamboo assisted by robotic fabrication. *Journal of Wood Science*, *66*(1), 1–11. https://doi.org/10.1186/s10086-020-01869-0
[11].Lorenzo, R., Mimendi, L., Yang, D., Li, H., Mouka, T., Dimitrakopoulos, E. G. (2021). Non-linear behaviour and failure mechanism of bamboo poles in bending. *Construction and Building Materials*, *305*, 124747. https://doi.org/10.1016/j.conbuildmat.2021.124747
[12].Mannan, S., Knox, J. P., Basu, S. (2017). Correlations between axial stiffness and microstructure of a species of bamboo. *Royal Society Open Science*, *4*(1), 160412. https://doi.org/10.1098/rsos.160412
[13].Mitch, D., Harries, K. A., Sharma, B. (2010). Characterization of splitting behavior of bamboo culms. *Journal of Materials in Civil Engineering*, *22*(11), 1195–1199. https://doi.org/10.1061/(ASCE)MT.1943-5533.0000120
[14].Moran, R., Webb, K., Harries, K., García, J. J. (2017). Edge bearing tests to assess the influence of radial gradation on the transverse behavior of bamboo. *Construction and Building Materials*, *131*, 574 – 584. https://doi.org/10.1016/j.conbuildmat.2016.11.106
[15].Mouka, T., Dimitrakopoulos, E. G. (2021). Simulation of embedment phenomena on bamboo culms via a modified foundation modelling approach. *Construction and Building Materials*, *275*, 122048. https://doi.org/10.1016/j.conbuildmat.2020.122048
[16].Mouka, T., Dimitrakopoulos, E. G., Lorenzo, R. (2022). Insight into the behaviour of bamboo culms subjected to bending. *Journal of the Royal Society Interface* (in press) https://dx.doi.org/10.1098/rsif.2021.0913.
[17].Paraskeva, T., Grigoropoulos, G., Dimitrakopoulos, E. G. (2017). Design and experimental verification of easily constructible bamboo footbridges for rural areas. *Engineering Structures*, *143*, 540 – 548. https://doi.org/10.1016/j.engstruct.2017.04.044
[18].Richard, M. J., Gottron, J., Harries, K. A., Ghavami, K. (2017). Experimental evaluation of longitudinal splitting of bamboo flexural components. *Proceedings of the Institution of Civil Engineers - Structures and Buildings*, *170*(4) 265–274. https://doi.org/10.1680/jstbu.16.00072
[19].Sharma, B., Harries, K. A., Ghavami, K. (2013). Methods of determining transverse mechanical properties of full-culm bamboo. *Construction and Building Materials*, *38*, 627 – 637, 25th Anniversary Session for ACI 228 – Building on the Past for the Future of NDT of Concrete. https://doi.org/10.1016/j.conbuildmat.2012.07.116
[20].Trujillo, D., Jangra, S., Gibson, J. M. (2017). Flexural properties as a basis for bamboo strength grading. *Proceedings of the Institute of Civil Engineers: Structures and Buildings*, *170*(4) 284–294. https://doi.org/10.1680/jstbu.16.00084
[21].Wang, X., Ren, H., Zhang, B., Fei, B., Burgert, I. (2012). Cell wall structure and formation of maturing fibres of Moso bamboo (*Phyllostachys pubescens*) increase buckling resistance. *Journal of The Royal Society Interface*, *9*(70), 988–996. https://doi.org/10.1098/rsif.2011.0462
[22].Wegst, U. G., Ashby, M. F. (2007). The structural efficiency of orthotropic stalks, stems and tubes. *Journal of Materials Science*, *42*(21), 9005–9014. https://doi.org/10.1007/s10853-007-1936-8
[23].Wu, W., Liu, Q., Zhu, Z., Shen, Y. (2015). Managing bamboo for carbon sequestration, bamboo stem and bamboo shoots. *Small-Scale Forestry*, *14*(2), 233–243. https://doi.org/10.1007/s11842-014-9284-4
[24].Young, W. C., Budynas, R. D. (2002). *Roark's formulas for stress and strain*, 7th Edition. McGraw-Hill, Two Penn Plaza, New York, NY 10121-2298.